

Precision and Uncertainty in the Characterization of Anisotropic Rotational Diffusion by ^{15}N Relaxation

Martin Blackledge,* Florence Cordier, Patrice Dosset, and Dominique Marion

Institut de Biologie Structurale, Jean-Pierre Ebel C.N.R.S.-C.E.A. 41, Avenue des Martyrs 38027 Grenoble Cedex, France

Received December 17, 1997

In this Communication we investigate the precision of the anisotropic diffusion tensor as determined by heteronuclear relaxation data. The analysis is applied to the cytochrome c_2 (cyt c_2) from *Rhodobacter capsulatus*. In recent years, heteronuclear NMR relaxation¹ has developed into an important method for probing fast internal dynamics in macromolecules. Data are commonly interpreted using the model-free formalism^{2,3} to give precise information concerning the flexibility of NH vectors in terms of an order parameter S^2 and a correlation time τ_i . In order for the model-free approach to give realistic information concerning local motions, a precise knowledge of the component of the autocorrelation function due to the overall tumbling of the molecule is necessary.⁴ It has been shown that the anisotropic diffusion tensor can be determined from the angular dependence of the relaxation of rigid regions of a protein, even in the case of relatively low anisotropy,^{5,6b} and that interpretation of heteronuclear relaxation using this formalism makes available previously inaccessible long-range structural information.⁷ It is therefore of interest to characterize the accuracy of the determination of the anisotropic diffusion tensor.

Experimental data consist of the direction cosines of the NH vectors under consideration, taken in this case from the NMR structure,⁸ the relaxation rate constants R_1 and R_2 , and their estimated uncertainties. Relaxation rate constants were determined using standard methods.⁹ For vectors undergoing low amplitude, rapid motions, the ratio R_2/R_1 is essentially independent of internal motion and is defined by the overall tumbling component of the spectral density function. Woessner has described the appropriate spectral density function for an asym-

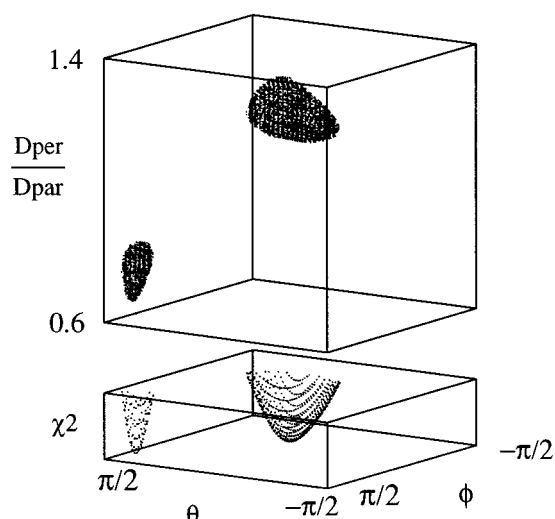


Figure 1. Representation of the error function $\chi^2 = \Sigma[(R_{2\text{meas}}/R_{1\text{meas}})^2 - (R_{2\text{sim}}/R_{1\text{sim}})^2]^2/\sigma^2$ with respect to the fitted parameter set for cyt c_2 . σ is the estimated experimental error. The lower matrix shows $\chi^2 < 30$ with respect to θ and ϕ (from $-\pi/2$ to $+\pi/2$). The upper matrix shows the $\chi^2 < 30$ region for θ , ϕ (over the same range) and D_{\perp}/D_{\parallel} (from 0.6 to 1.40).

metric top with an anisotropic diffusion tensor.¹⁰ In the case of a generally anisotropic tensor, six parameters (D_{xx} , D_{yy} , D_{zz} , θ , ϕ , ψ) are optimized, where the Euler angles define the orientation of the diffusion tensor frame in the chosen molecular frame. In the simpler axially symmetric model four parameters are optimized (D_{\perp} , D_{\parallel} , θ , ϕ). In all cases, the six or four parameters are extracted by minimizing the error function χ^2 representing the difference between experimental and predicted R_2/R_1 ratios for a selection of comparatively rigid vectors. The cyt c_2 (116 residues) is particularly well suited to this study, comprising six helical segments (44 NH vectors) sampling a large range of orientations.

The parametric space available for the determination of the axially asymmetric diffusion tensor by minimization of χ^2 is illustrated in Figure 1 for the case of the cyt c_2 . In general, when a truly anisotropic system is approximated by the simpler axially asymmetric tensor, two minima can exist, with the unique axes corresponding approximately to the largest and smallest components of the diffusion tensor. However the exact form of the χ^2 hypersurface depends on the nature of the diffusion tensor, the distribution of vectors in the molecule and the coherence of the relaxation data. In the case of the cyt c_2 there exist two similarly significant well-defined minima representing prolate and oblate approximations to the real, more complex form of the molecule. Note the significantly reduced angular dispersion in the prolate approximation (Figure 2) resulting in a narrower minimum in angular space (Figure 1).

The fit of the diffusion tensor proposed here uses a highly efficient simulated annealing algorithm¹¹ developed in our laboratory. This allows extensive exploration of the available parametric space, facilitating the application of sufficiently sampled Monte Carlo (MC) simulations to evaluate the uncertainty of the fitted diffusion parameters, and the significance of the improved fit. For each fit (four or six parameters), 500 $\{R_1, R_2\}$ datasets have been simulated for all residues under consideration. These datasets were selected from a Gaussian noise distribution centered on the optimal rates back-calculated from the best fit anisotropic diffusion parameters and representing the estimated R_1 and R_2 uncertainties.

* To whom correspondence should be addressed.

(1) Abragam, A. *The Principles of Nuclear Magnetism*; The International Series of Monographs on Physics; Oxford University Press: Oxford, 1961.

(2) Lipari, G.; Szabo, A. *J. Am. Chem. Soc.* **1982**, *104*, 4546–4558, 4559–4570.

(3) Clore, G. M.; Szabo, A.; Bax, A.; Kay, L. E.; Driscoll, P. C.; Gronenborn, A. M. *J. Am. Chem. Soc.* **1990**, *112*, 4989–4991.

(4) Brüschweiler, R.; Liao, X.; Wright, P. E. *Science* **1995**, *268*, 886–889.

(5) (a) Barbato, G.; Ikura, M.; Kay, L. E.; Pastor, R. W.; Bax, A. *Biochemistry* **1992**, *31*, 5269–5278. (b) Tjandra, N.; Feller, S. E.; Pastor, R. W.; Bax, A. *J. Am. Chem. Soc.* **1995**, *117*, 12562–12566. (c) Hansen, A. P.; Petros, A. M.; Meadows, R. P.; Fesik, S. W. *Biochemistry* **1994**, *33*, 15418–15424. Tjandra, N.; Koboniwa, H.; Ren, H.; Bax, A. *Eur. J. Biochem.* **1995**, *230*, 1014–1024. Zheng, Z.; Czaplicki, J.; Jardetzky, O. *Biochemistry* **1995**, *34*, 5212–5223. Broadhurst, R. W.; Hardman, C. H.; Thomas, J. O.; Laue, E. D. *Biochemistry* **1995**, *34*, 16608–16617. Tjandra, N.; Wingfield, P.; Stahl, S.; Bax, A. *J. Biomol. NMR* **1996**, *8*, 273–284. Mackay, J.; P.; Shaw, G. L.; King, G. F. *Biochemistry* **1996**, *35*, 4867–4877. Luginbühl, P.; Pervushin, K. V.; Iwai, H.; Wüthrich, K. *Biochemistry* **1997**, *36*, 7305–7312.

(6) (a) Kördel, J.; Skelton, N. J.; Akke, M.; Palmer, A. G.; Chazin, W. J. *Biochemistry* **1992**, *31*, 4856–4866. (b) Lee, L. K.; Rance, M.; Chazin, W. J.; Palmer, A. G. *J. Biomol. NMR* **1997**, *9*, 287–298.

(7) Tjandra, N.; Garrett, D. S.; Gronenborn, A. M.; Bax, A.; Clore, G. M. *Nat. Struct. Biol.* **1997**, *4*, 443–449.

(8) NMR structure coordinates will be deposited in the Brookhaven database—the NH coordinates and relaxation rates can be found in the Supporting Information.

(9) Farrow, N. A.; Muhandiram, R.; Singer, A. U.; Pascal, S. M.; Kay, C. M.; Gish, G.; Shoelson, S. E.; Pawson, T.; Forman-Kay, J. D.; Kay, L. E. *Biochemistry* **1994**, *33*, 5984–6003. Peng, P. W.; Wagner, G. *J. Magn. Reson.* **1992**, *98*, 308–332.

(10) Woessner, D. E. *J. Chem. Phys.* **1962**, *3*, 647–654.

(11) Metropolis, N.; Rosenbluth, A.; Rosenbluth, M.; Teller, A.; Teller, E. *J. Chem. Phys.* **1953**, *21*, 1087–1094.

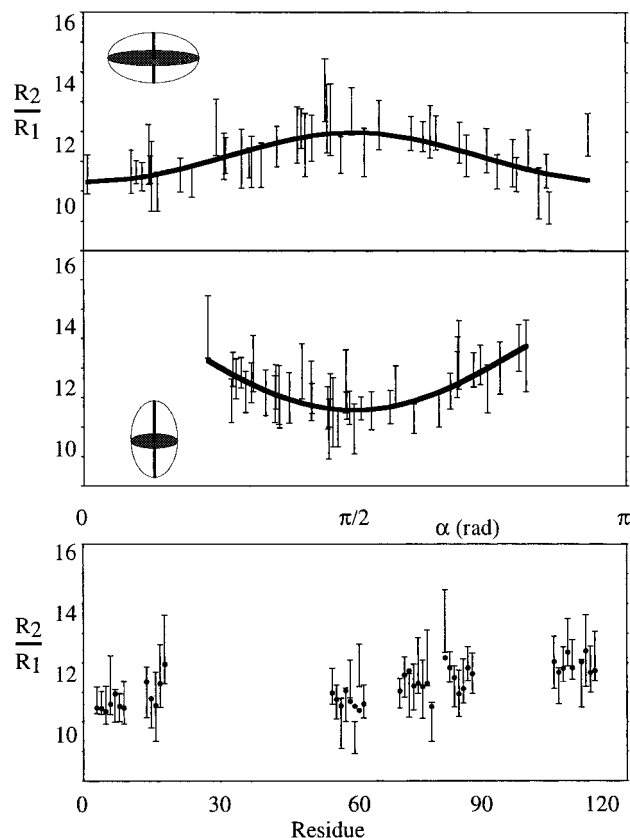


Figure 2. Fit of anisotropic diffusion tensor for cyt c_2 . (a) (top) Dependence of the observed (points with error bars) and simulated (solid line) R_2/R_1 ratios on the angle between the NH vector and the unique axis of the diffusion tensor for minimum m_1 ($D_{\perp}/D_{\parallel} = 0.84 \pm 0.02$). (b) (middle) As Figure 2a for minimum m_2 ($D_{\perp}/D_{\parallel} = 1.34 \pm 0.05$). (c) (bottom) Results of six-parameter fit using a fully anisotropic diffusion tensor. Observed data (centered on error bars) and simulated (circles) R_2/R_1 ratios for the 44 fitted residues in helical regions.

The χ^2 distributions derived from simulated datasets from the two four-parameter minima m_1 and m_2 shown in (Figure 1) exhibit similar behavior—in both cases the χ^2_{exp} is acceptable within 95% confidence limits as determined from the simulated datasets, justifying both prolate and oblate models.¹² In both cases the orthogonal minima are sparsely populated (5/500 and 3/500) by the MC data, demonstrating the definition of the two solutions. Within the MC datasets we find a significant anticorrelation between D_{\perp} and D_{\parallel} (data not shown) due to the need to preserve a well-defined $D_{\text{iso}} = (2D_{\perp} + D_{\parallel})/3$ despite the large variation of D_{\perp} and D_{\parallel} .

The fully anisotropic fit lowers the χ^2_{exp} ,¹² this is again lower than the 95% confidence limit defined by the simulated datasets and qualitatively improves the fit. The accuracy of the fit is illustrated by the reproduction of the periodic nature of the relaxation in the helices (Figure 2c). The two orthogonal unique axes found for the axial minima m_1 and m_2 are approximately reproduced by the two components D_{zz} and D_{yy} .

We have evaluated the significance of the improved fit using the fully anisotropic tensor, compared to the random statistical reduction in χ^2_{exp} gained from introduction of two supplementary parameters, by treating each simulated data set back-calculated from the 4-parameter fit minima, with both 4- and 6-parameter

fits. The improvement in the fit due to the fully anisotropic model is found to be significant irrespective of the true number of degrees of freedom available.¹² This can however be estimated from the χ^2 distributions to be significantly lower than the expectation value assuming independent vectorial orientation (22–24 compared to 38–40).

A similar analysis has been performed for published data from Calbindin D_{9k} , recently the subject of a detailed study of anisotropic diffusion.⁶ We find that this dataset also exhibits geometrically orthogonal minima with very similar χ^2_{exp} . The MC simulated datasets populate the orthogonal minima to a greater extent than for the cyt c_2 —possibly reflecting less well-defined anisotropy. This is confirmed by the χ^2_{exp} which is higher than the MC derived confidence limit for statistical acceptance.¹³ The relative definition of the minima can be estimated by comparing the χ^2 with respect to randomly assigned relaxation rates^{5b} and χ^2_{exp} : in the case of cyt c_2 the latter is a factor 2 smaller and a factor 1.2 smaller for Calbindin χ^2_{exp} . Note that the Calbindin study treated a selection of vectors identified from their relaxation properties as exhibiting no obvious internal mobility or exchange (60/75), while the cyt c_2 topology allowed us to define a more restrained dataset based on independent structural criteria, containing only residues in helical motifs. The relatively high definition of the cyt c_2 data probably stems from the large angular distribution present in the dataset and the rigid structural motif common to all treated vectors.

In conclusion, we have investigated in detail the error function associated with the fit of the anisotropic diffusion tensor to heteronuclear relaxation data. Care must be taken when interpreting the results of multiparameter fits assuming axially symmetric anisotropy in the case of fully anisotropic molecules as more than one minimum may be present in the conformational space. The use of a highly efficient minimization algorithm allows a robust determination of significance and a reasonable estimation of uncertainties in the parameters defining the diffusion tensor. While it has previously been proposed that the fully anisotropic diffusion tensor is not statistically acceptable, we find that for the cyt c_2 this description is justified both qualitatively and quantitatively and is therefore necessary for the detailed interpretation of the internal mobility of the molecule. In general the presence of two equally significant minima carries the implication that a more complex model is required. A more detailed investigation shows that incorporation of the optimized asymmetric diffusion tensor into a Lipari–Szabo type analysis of R_1 , R_2 and NOE provides an improved description of the internal mobility of the cyt c_2 , compared to both isotropic and axially anisotropic tensors.¹⁴ Using this description, the overall precision of the fit increases, and a larger proportion of residues are coherent with the model-free approach. Using the simpler tensorial models fictitious internal mobility may be evoked to account for residual rotational anisotropy. Finally, structure calculations which exploit the angular dependence of relaxation data using an axially symmetric model for fully asymmetric molecules will clearly provide less-precise refinement than a model using all three available axes.

Supporting Information Available: A listing of NH vector coordinates and relaxation rates for cyt c_2 and a full analysis of cyt c_2 and Calbindin D_{9k} (9 pages, print/PDF). See any current masthead page for ordering information and Web access instructions.

JA9742646

(13) $\chi^2_{\text{exp}} = (79.3, 79.4), (84.3, 90.6)$, for orthogonal minima fitted with X-ray or NMR structures, respectively. $\chi^2_{0.05} = (72.9, 71.1)$ and $(75.6, 74.3)$ for the same datasets. The unusually high χ^2_{exp} have already been noted by the authors of the previous study.⁹ Supporting Information contains full details of the statistical analysis of Calbindin D_{9k} .

(14) Cordier, F.; Caffrey, M.; Brutscher, B.; Cusanovich, M.; Marion, D.; Blackledge, M. Submitted.

(12) The Supporting Information contains full details of the statistical analysis. $\chi^2_{\text{exp}} = (24.6, 25.1)$ and $\chi^2_{0.05} = (34.7, 34.2)$ for orthogonal minima m_1, m_2 , respectively. For a fully anisotropic fit, $\chi^2_{\text{exp}} = 21.4$ and $\chi^2_{0.05} = 33.6$.